Simulation of classification in a gravitational inertial air classifier using a fast CFD-DPM approach method

Horacio A. Petit[1*], Erick Guimaraes[1], Luis Marcelo Tavares[1]

[1]Department of Metallurgical and Materials Engineering, Universidade Federal do Rio de Janeiro – COPPE/UFRJ, Rio de Janeiro, RJ, Brazil

Abstract. This work presents a fast CFD-DPM simulation approach for the simulation of a gravitational-inertial classifier, as operated in a gneiss quarry. Industrial surveys were carried out to gather data on the classifier performance under different operating conditions. The simulation approach consisted in the simplification of a CFD-DPM workflow to address the reduction of the computation time required to obtain a good representation of the classification performance. For this purpose, the simplification of the computational domain as well as a coarse graining approach were used to reduce the number of particles in the simulations and obtain results in an affordable computation time, presenting fairly accurate results compared to the industrial data.

1. Introduction

In the minerals industry, air classification is mainly used when the moisture content of the materials is low. The aggregate industry is a very good example, using air classification after crushing and sieving units to remove fine particles (Petit et al., 2018). Different designs of air classifiers are available (Shapiro and Galperin, 2005). Among them, the Gravitational-Inertial Classifier (GIC) has been adopted in the aggregate industry, drawing the attention of the academic community which started to study the classifier using experimental and numerical techniques (Johansson and Evertsson 2012a, 2012b).

The GIC presents a complex airflow, presenting two air inlets that can be adjusted to modify the contribution of each inlet on the overall airflow. The two airflows merge in the chamber passing through a set of classification channels designed to create a certain balance between gravity and centrifugal force on the particles. Also, it presents a recirculation zone where particles that were not classified have a second chance of reporting to either the coarse or the fine fractions.

The complexity of the air-laden flow inside the GIC chamber present a perfect case of study for computational modelling applications. In this regard, previous studies used a Eulerian-Eulerian Computational Fluid Dynamic (EECFD) approach to describe the air-laden flow inside the GIC (Johansson and Evertsson, 2012b). Other methods such as the Discrete Element Phase (DPM) or the Discrete Element Method (DEM) could be coupled to CFD solvers to recreate the particle trajectories inside the GIC chamber. However, the main issue seems to be the number of particles required to recreate the wide Particle Size Distribution (PSD) of the feed. Additionally, particles in the simulation should exchange momentum with the fluid phase to model the pressure loss. In this regard, attempts to reduce the number of particles without accounting for the momentum exchange may result in poor resolution of the airflow and the classification performance. Thus, no previous attempts of using Eulerian-Lagrangian CFD (ELCFD) approaches to simulate the performance of the GIC have been published.

This work proposes a fast CFD-DPM simulation approach to obtain fairly accurate estimations of the performance of a gravitational inertial classifier in an affordable computation time. The subject of study is a GIC operating in a gneiss quarry. The fast simulation approach is based on the simplification of the computational domain and the utilization of a coarse graining method to reduce the number of simulated particles while still accounting for the effect of solids loading on the classification performance. Data, gathered during a field campaign at the industrial site, were also used for setting boundary conditions and for validation.

2. Materials and Methods

The GIC is installed in a gneiss quarry located in the metropolitan area of Rio de Janeiro. The quarry possesses three crushing schemes. The output of the tertiary crusher (VSI) is sent to a double screen deck, whose undersize (< 2.36 mm) is fed to the GIC (Fig. 1). The coarse product of the classifier is conveyed to a silo where it is stocked for later shipment. The fine product of the GIC is sent directly to a bag filter with no intermediate classification or dedusting equipment. The classifier presents a primary airflow that enters the separator at the top, and a secondary airflow that enters the equipment at the bottom.

The classifier performance is tuned by setting the overall flow rate, by means of a frequency controller

* Corresponding author: hpetit@metalmat.ufrj.br

linked to the fan power input and by adjusting the primary and secondary air valves. As such, different contributions of the primary and secondary airflows change the air velocity inside the classification chamber, modifying the classification performance.

An industrial campaign was carried out to characterize the fluid dynamics conditions and classification performance of the GIC as used at the site. Air static pressure and velocity were measured by setting probes in the primary inlet, secondary inlet, and outlet of the GIC (Fig. 1). The classification performance was changed by setting different conditions of the primary and secondary air valves, using a 2^2 design of experiments presented with central point, shown in Table 1. The nominal fan frequency of 1800 rpm was used in all cases.

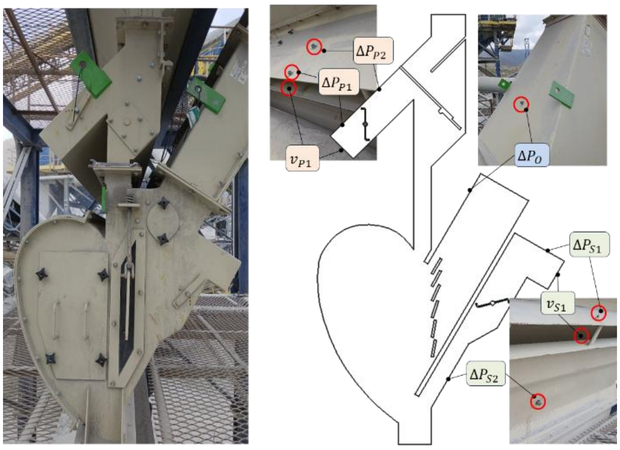

Fig. 1: Gravitational-inertial classifier (left), pressure and velocity probe locations used on site (right).

Table 1: Design of experiments carried out during industrial campaign

Test	Primary airflow	Secondary airflow	Case
1	Minimum	Minimum	Min - Min
2	Maximum	Minimum	Max -Min
3	Minimum	Maximum	Min - Max
4	Medium	Medium	Mid - Mid
5	Maximum	Maximum	Max - Max

The fast CFD-DPM method used to simulate the GIC performance was executed using Ansys Fluent capabilities. The computational domain representing the GIC chamber was reduced to a 50 mm slice, as presented in Fig. 2. Only the most important features of the geometry were represented. Air was modelled using the RANS equations. Boundary conditions for the air were computed based on the mean average values obtained during the industrial campaign. Velocity values at the primary and secondary physical inlets were used to compute the mean velocity downstream at the computational model inlets.

Gneiss particles entering the classifier were simulated using the DPM method. DPM groups particles of same sizes in groups called parcels. The trajectory of each parcel is tracked in the domain considering the force balance equations of a single particle but carrying the mass of the hole cluster of particles. This approach reduces the number of elements tracked in the simulation. Parcels do not interact with each other, and the volume of the particles is not accounted in the simulations.

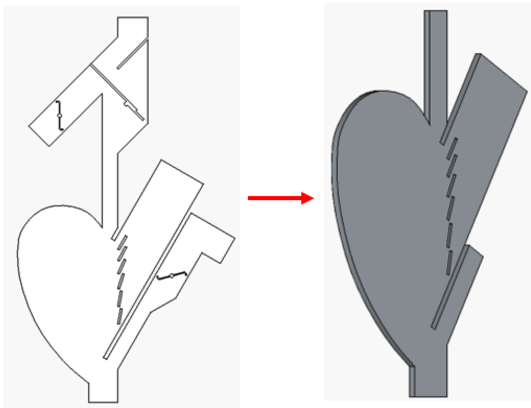

Fig. 2: CAD of the full GIC geometry (left), sliced simplified domain used in the CFD-DPM simulations (right).

In principle, the number of parcels in the domain is too high for the simulation to run in an affordable time. This is due to the wide PSD of the feed and the necessity of simulating fine particles to have a good representation of the classification, which is expected to present cut sizes near 75 µm. In this regard, a coarse graining method was used to simulate the bulk behaviour of the particles inside the classification chamber. The wide PSD of the feed was replaced by particles presenting a single particle size. The density of the particles was maintained to conserve mass and volume. The size of the particles was computed to conserve the momentum exchange inside the chamber, calculated based on an estimation of particle and air velocities in the classification region. The coarse graining size resulted in 1 mm, presenting a reduction of the particle number of 92%. The computation of the partition curve was performed by adding a pulse of tracer parcels into the simulation. Tracer particle sizes covered the wide range of the feed PSD but with an arbitrary small feed rate; thus, with a small contribution in the overall number of particles added into the simulation.

The simulation of the classification started by simulating the fluid flow until stable velocity and pressure conditions were achieved. Then, bulk particles with the coarse graining size were injected into the simulation. The simulation was resumed until new stable conditions were achieved. Finally, tracer particles were injected into the simulation. The simulations were continued until classification of tracer particles were achieved.

3. Results and discussion

Results of the industrial campaign, in terms of the total flow rate and pressure loss of the GIC are presented in Fig. 3. Total airflow and pressure loss depends on the positions of the air valves and the feed of particles, as expected. The min–min case presents the lowest airflow and the highest pressure loss, while the max–max case presents the opposite condition. Airflow and pressure losses are influenced by the presence of solid particles fed to the classification process, as observed in the air-laden conditions. Pressure loss increases due to the presence of particles, while airflow reduces, as expected. The overall results present consistent behaviour with a small deviation in the mid-mid case, which presents lower airflow and higher pressure flow compared to the overall trend in the results.

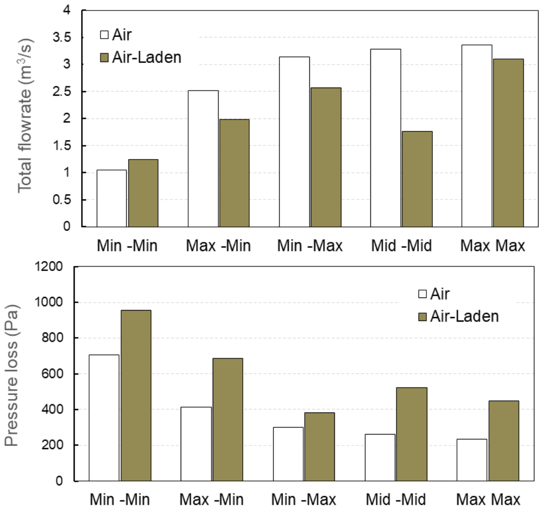

Fig. 3: Experimental results for the study cases in terms of the total airflow (top), and pressure loss (bottom).

Results of the CFD simulations in terms of the air velocity magnitude are presented in Fig. 4 for the min-min and max-max cases. Results show the large differences in the velocity field inside the chamber depending on the positions of the air valves. Max-max case presents a more intense flow field and greater contribution of the secondary airflow. Fig. 4 also presents the results of the velocity field after injection of the particles. The effect of the solid loading is clearly visible in both cases, but more evident in the max-max case due to the interference with the more intense recirculation flow near the internal deflectors.

The effect of solids loading on the fluid flow inside the chamber is more evident in the results presented in Fig. 5. Pressure loss is plotted as a function of time for two selected study cases. Particles are injected in the simulation at 3 s, where a jump in the pressure loss occurs. As observed, CFD-DPM simulations can reproduce the effect of solid loadings but differences in the results are clear when compared to the presented experimental values. The min-min case presented considerable errors even in the absence of particles, while the max-max case presented fair representation of the experimental results for both the air and air-laden conditions.

Snapshots of instantaneous particle positions for two selected cases are presented in Fig. 6. The classification mechanism inside the chamber is clearly observed in both cases. Bulk particles (size ≈ 1 mm) descend through the chamber with negligible action because of air drag. Bulk particle trajectories are hardly modified even when passing through the secondary inlet at the bottom. Thus, recirculation of bulk particles because of the secondary inlet is not represented, being a limitation of the modelling approach. Despite the apparent disconnection between air and particles, the pressure loss jump presented in Fig. 5 evidence that air-particle interactions are properly accounted for in the model.

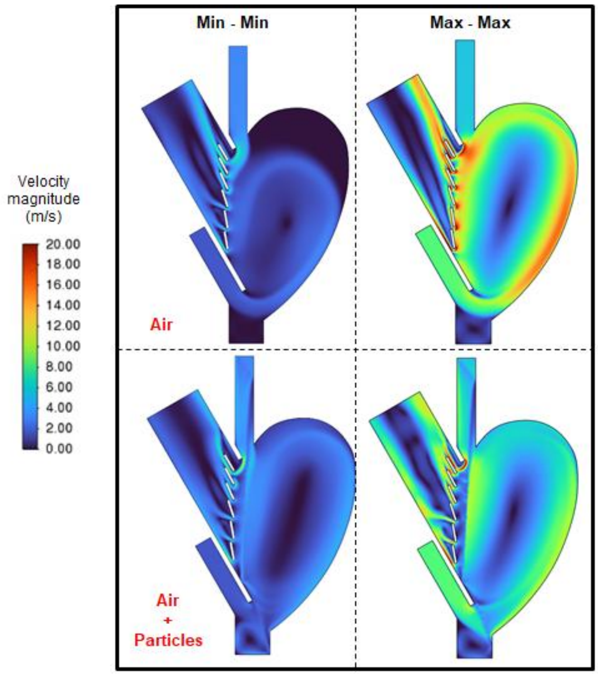

Fig. 4: CFD velocity results (top) vs CFD-DPM results (bottom) for two of the study cases.

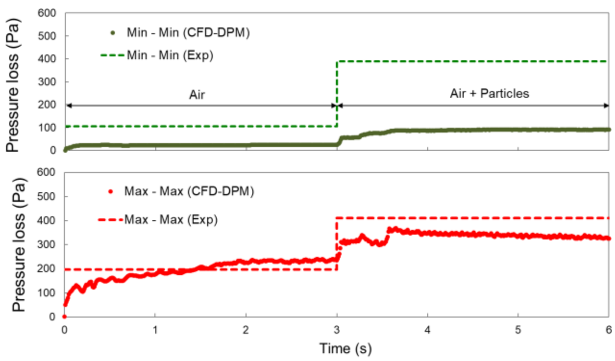

Fig. 5: CFD-DPM results in terms of particle positions for two of the study cases.

The trajectories of tracer parcels (sizes ≤ 1 mm) are presented in Fig. 6, describing the classification inside the GIC. Comparison between the min-min and max-max cases present differences in the particle sizes that are dragged to the outlet of the classifier. Fig. 7 presents the classification performance in terms of the partition curves for two selected cases. Experimental results show that the cut size is near 75 μm for the max-max case, being the higher cut size found among the study cases. Other cases, such as the min-min case, present cut sizes finer than 50 μm. Such fine cut sizes suggest that the GIC is operating at airflow rates lower than designed. Comparison between experimental and numerical results demonstrate that CFD-DPM results presents classification performance close to ideal, with an overestimated sharpness of cut and neglecting the fishhook effect for the finer sizes.

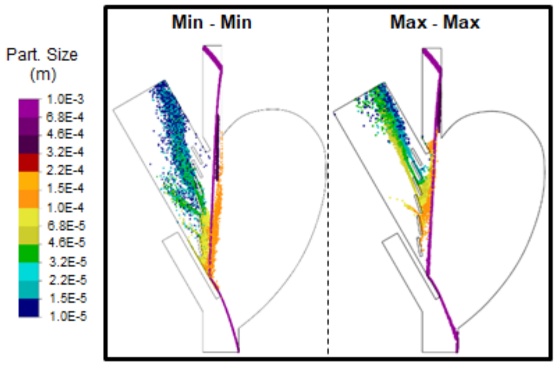

Fig. 6: CFD-DPM results in terms of particle positions for two of the case studies.

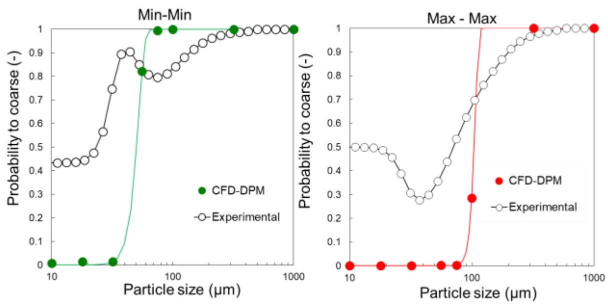

Fig. 7: Comparison between experimental and predicted partition curves for two selected case studies.

Differences between simulated and experimental results were expected as the fast CFD-DPM approach was proposed to give fast simulation results at the risk of neglecting secondary but important physical behaviors such as the account of solids volume fraction inside the chamber or the adhesion / cohesion forces that affect classification of fine particles due to particle clustering. Such phenomena may be represented in more ambitious simulation approaches, but that demand considerably higher computation times.

Despite the evident errors, Fig. 8 shows good agreement between simulated and experimental results when comparing the x_{80} of the case studies. The value of x_{80} may seem arbitrary, but the x_{50} value could not be computed in some of the cases. Despite the simulation deviations, Fig. 8 shows that the fast CFD-DPM approach represents the trend in the x_{80}, proving that the method can be used to simulate industrial scenarios maintaining internal consistency and being of value to spot the effect of operating variables on classification performance.

Computation time resulted in approximately 60 hours using a workstation featuring an AMD Ryzen 2920X (12 Cores) and 64 GB of RAM, which is an affordable computation time, considerably shorter than a similar simulation using standard CFD-DEM methods in the same workstation.

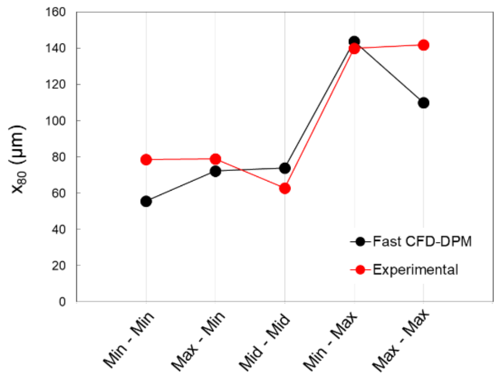

Fig. 8: Summary of experimental versus predicted x_{80}.

4. Conclusions

A fast CFD-DPM simulation approach was used for the simulation of the classification of gneiss particles in an industrial GIC.

The method was able to give fairly accurate results when predicting the overall pressure loss with and without particles being fed to the process.

Partition curves obtained with the method present closer to ideal classification due to the physical effects neglected in order to accelerate the computation of the method.

Despite the deviations in prediction of the partition curves, the method showed consistent results preserving the trends in the experimental results.

Acknowledgement

The authors want to thank the Brazilian research agencies CNPq and FAPERJ as well as to Mineração Santa Luzia for the support in the making of the present work.

References

Shapiro M., Galperin V. (2005). Air classification of solid particles: a review, Chem. Eng. Proc. 44 (2005) 279-285.

Petit H. A., Cordoba G., Paulo C. I., Irassar E. F. (2018) Novel air classification process to sustainable production of manufactured sands for aggregate industry. J. of Cleaner Production. 198 (2018) 112-120.

Johansson R., Evertsson M. (2012a) An empirical study of a gravitational air classifier. Minerals Engineering. Vol 31 10-16.

Johansson R., Evertsson M. (2012b) CFD simulation of a gravitational air classifier. Minerals Engineering. Vol 33 20-26.